Large-scale electronic-structure theory and nanoscale defects formed in cleavage process of silicon

T. Hoshi *,[a,b] R. Takayama [c,1] Y. Iguchi [a] T. Fujiwara [a,b]

[a] *Department of Applied Physics, University of Tokyo, Tokyo, Japan*
[b] *Core Research for Evolutional Science and Technology (CREST), Japan Science and Technology Agency, Saitama, Japan.*
[c] *Research and Development for Applying Advanced Computational Science and Technology (ACT-JST), Japan Science and Technology Agency, Saitama, Japan.*

Abstract

Several methods are constructed for large-scale electronic structure calculations. Test calculations are carried out with up to 10^7 atoms. As an application, cleavage process of silicon is investigated by molecular dynamics simulation with 10-nm-scale systems. As well as the elementary formation process of the (111)-(2 × 1) surface, we obtain nanoscale defects, that is, step formation and bending of cleavage path into favorite (experimentally observed) planes. These results are consistent to experiments. Moreover, the simulation result predicts an explicit step structure on the cleaved surface, which shows a bias-dependent STM image.

Key words: order-N electronic-structure theory, nanoscale defect, surface process of silicon, bias-dependent STM image.

1. Introduction

Quantum mechanical (electronic structure) calculation with 10-nm-scale systems is of great importance in the present semiconductor technology. Particularly, dynamical simulations are highly desirable so as to explore industrial processes. These simulations, however, are quite difficult for the present standard methodology, such as the Car-Parrinello method (1), owing to its heavy computational cost. So as to overcome the difficulty, methodology for large systems, with thousands of atoms or more, has been focused from 1990's. (2; 3) Its mathematical foundation is the calculation of one-body density matrix, instead of one-electron eigenstates. In this paper, we will show the investigation of nanoscale defects formed in cleavage process of silicon (4), which is an example of our newly-developed practical methods of large-scale electronic structure calculations. (5; 6; 7; 8; 9; 10) These methods are general and are applicable to not only single-atom defects but also nanoscale defects.

2. Theory

The foundation of the large-scale electronic structure calculation was established by W. Kohn (2). Any physical quantity X can be given by the one-body density matrix ρ as

$$\langle \hat{X} \rangle = \mathrm{Tr}[\hat{\rho}\hat{X}] = \int\int d\boldsymbol{r} d\boldsymbol{r}' \rho(\boldsymbol{r}, \boldsymbol{r}') X(\boldsymbol{r}', \boldsymbol{r}), \qquad (1)$$

where the density matrix is defined, from occupied one-electron eigenstates $\phi_k(\boldsymbol{r})$, as

* corresponding author
Takeo Hoshi
University of Tokyo
7-3-1 Hongo, Bunkyo-ku, Tokyo, Japan
tel +81-3-5841-6812; fax +81-3-5841-6869
Email address: hoshi@coral.t.u-tokyo.ac.jp (T. Hoshi).
URL: http://fujimac.t.u-tokyo.ac.jp/lses/ (T. Hoshi).
[1] Present address:Canon Inc., Analysis technology center, 30-2 Shimomaruko 3-Chome, Ohta-ku, Tokyo 146-8501, Japan

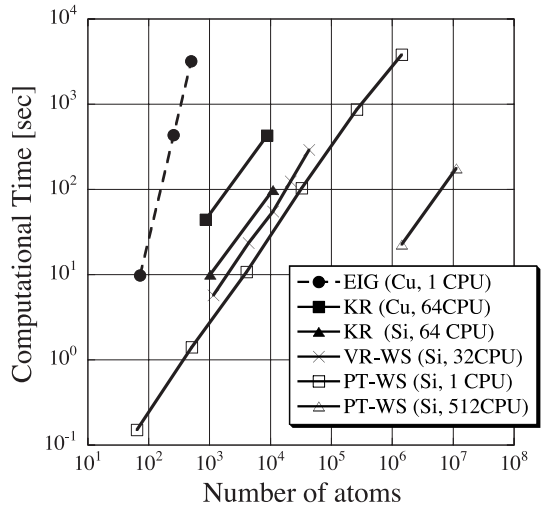

Fig. 1. The computational time for bulk Si or Cu as a function of the number of atoms (N), up to 11,315,021 atoms (Refs. (7; 4) and this work). The time was measured for electronic structure calculation with a given atomic structure. The calculations were carried out by the conventional eigenstate calculation (EIG) and by our methods for large system; (i) Krylov-subspace method (KR) with subspace-diagonalization procedure, (ii) variational Wannier-state method (VR-WS) and (iii) perturbative Wannier-state method (PT-WS). For '1CPU' computations, we used single Pentium 4$^{\rm TM}$ processor in 2 GHz. Parallel computations were carried out by SGI Origin 3800$^{\rm TM}$ (for PT-WS method), Origin 2800$^{\rm TM}$ (for VR-WS method) and Altix 3700$^{\rm TM}$ (for KR method).

$$\hat{\rho} = \sum_{k}^{\rm occ.} |\phi_k\rangle\langle\phi_k|. \qquad (2)$$

The most important fact is that, in case that $\hat{X}$ is a short-range operator, the physical quantity $\langle\hat{X}\rangle$ is contributed only by the short-range component of the density matrix, even though the density matrix $\rho(\boldsymbol{r}, \boldsymbol{r}')$ is of long range. Owing to this fact, W. Kohn proved that the density-functional (*ab initio*) theory can be constructed from the short-range component of the density matrix, instead of eigenstates (Kohn-Sham orbitals).

Another methodological foundation for large-scale calculation is the transferable Hamiltonians in the Slater-Koster (tight-binding) form. They are of short range and applicable to various circumstances, *e.g.*, crystals, defects, liquid and surfaces. Their success has been known for decades and can be founded by the *ab initio* theory. (15)

For practical large-scale calculations, we have developed a set of theories and program codes with obtaining density matrix. They are founded by generalized Wannier state (5; 6; 7; 4) or Krylov subspace (Refs. (13; 9; 10) and this work). These methods are calculation methods for short-range component of the density matrix with a given Hamiltonian. A bench mark is shown in Fig. 1, in which the computational time of our methods, unlike that of the conventional eigenstate calculation, is 'order-N', or linearly proportional to the system size (N). Here and hereafter, all the calculations of Si are carried out using a typical transferable Hamiltonian. (12) For the present calculation of Cu, we used the Slater-Koster type Hamiltonian constructed from in the LMTO theory (14).

As well as the calculation methods for density matrix, we also constructed a method for Green function of large systems, which is based on Krylov subspace. (10; 11)

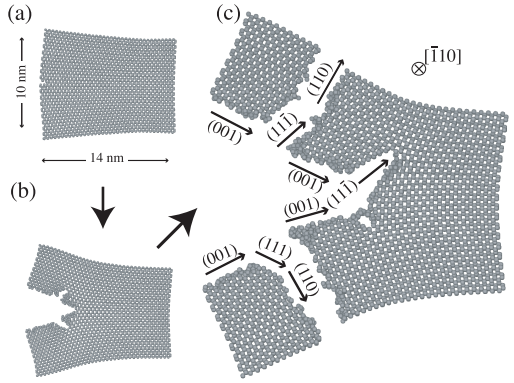

Fig. 2. Bending of cleavage path into the favorite (experimentally observed) planes, (111) and (110) planes. (4) The time interval Δt between the snapshots (a) and (b) and that between (b) and (c) are $\Delta t = 1$ ps and 2 ps, respectively.

3. Application to cleavage process in silicon

As the first application of our method, we focused on the cleavage process of silicon. Molecular dynamics simulations were carried out with 10-nm scale samples or with upto 10^5 atoms. (7; 4)

Since cleavage is a nonequilibrium process with a typical velocity scale of propagation velocity, its dynamical mechanism is essential. (16; 17) Although cleavage process was simulated with electronic structure thus far, (18; 19) its investigation was quite limited, owing to its small system size of 10^2 atoms. The present simulation method enables investigation beyond the above limitation.

Numerical accuracy of the present simulation was confirmed, not only in elastic constants and surface energy, but also in the following quantities that can be measured by cleavage experiments; (i) The critical stress intensity factor for cleavage $K_{\rm c}$ was evaluated to be $K_{\rm c} = 0.7{\rm MPa}\sqrt{\rm m}$, which agrees well with experimental values of $K_{\rm c} = 0.65 - 1.24{\rm MPa}\sqrt{\rm m}$. (18) (ii) The cleavage propagation velocity was evaluated to be $v \approx 2$nm/ps=2km/s, which agrees well with a recent experimental value of $v = 2.3 \pm 0.3$km/s. (20)

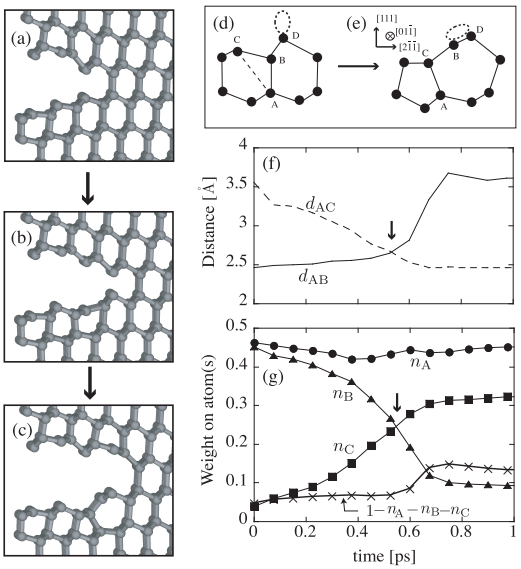

Fig. 3. Elementary surface reconstruction process in silicon cleavage with (111) − (2×1) surface. (4) (a)-(c) : Snapshots of process. (d)-(e) : Schematic figures of (d) the buckled (2 × 1) structure that appears in the snapshot (b) and (e) the π-bonded (Pandey) (2×1) structure that appears in the snapshot (c). The oval indicates the presence of a doubly occupied surface state. (e)-(f): Quantum mechanical analysis of a process in which the bonding wavefunction (ϕ_i) between A and B sites changes into that between A and C sites ($A-B \Rightarrow A-C$); Figure (f) shows the interatomic distances d_{AB} and d_{AC}. Figure (g) shows the occupation weight on the A, B and C atom sites (n_A, n_B, n_C) for the wavefunction ϕ_i. A typical transitional state, with $d_{AB} \approx d_{AC}$ or $n_B \approx n_C$, appears at the time marked by arrows in (f) and (g).

3.1. *Bending of cleavage path into favorite planes*

Experimentally, the cleavage plane of silicon is the (111) plane with a metastable (2 × 1) reconstruction or the (110) plane (less favorable). (22) The appearance of these cleaved surfaces cannot be explained from the traditional approach with surface energy. As a fruitful result of the present 10-nm-scale simulation, the experimental preference of cleaved surfaces is reproduced by bending of cleavage path; As a typical result, Fig. 2 shows that, even if the cleavage initiates artificially on another plane ((001) plane), the cleavage path is bent into the experimentally observed planes ((111) and (110) planes). Moreover, we obtained a well-defined surface reconstruction on the (111) and (110) planes after bending (4).

3.2. *Stable cleavage mode on* (111) *surface with* (2×1) *reconstruction*

Our simulation results reproduce the stable (experimental) cleavage mode with the π-bonded (111)-(2×1) surface that was proposed first by Pandey (21) and is currently well established in both experiment and theory. (22) Since a surface atom on the *ideal* (111) surface has one dangling-bond electron, the pairing mechanism between the nearest neighbor dangling-bond electrons is the motive force of the surface reconstruction. Figure 3 shows the actual reconstruction process with quantum mechanical analysis of the wavefunction. The resultant surface contains a pair of five- and seven-membered rings as the unit of the π-bonded (2 × 1) structure. The π-bonding appears between the B and D sites in Fig. 3(e), as indicated by an oval.

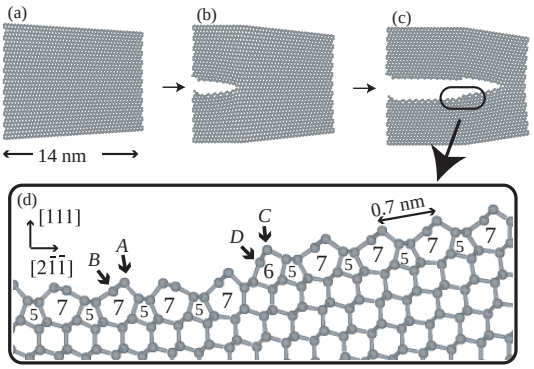

Fig. 4. Stable (experimentally observed) cleavage mode on (111) − (2×1) surface. (4) (a)-(c):Successive snapshots with a time interval of approximately Δt = 4ps. (d) : Close up of the snapshot (c), in which a step structure with a six-membered ring appears.

3.3. *Step structure and bias-dependent STM image*

In our results, step formation were frequently observed on the (111)-(2 × 1) surface. The frequently observed step appears in Fig. 4(d) and has a six-membered ring at the step edge. The formation process was investigated with quantum mechanical (electronic) freedom and we found the mechanism that explains why this kind of step appears so frequently. (4) Among STM experiments on cleaved surface, on the other hand, several step structures were observed but their explicit atomic structures have not been settled. (23; 24; 25) Since our results were independent from the experiments, we propose the present step structure as a hopeful candidate.

So as to compare with STM experiments, the local density of states (LDOS) was calculated for the surface atoms, the A, B, C, D sites in Fig. 4(d), using the Krylov subspace method for Green function. (10; 11) In result, the upper (vacuum side) atom (A or C site) has an *occupied* surface state and the lower (bulk side) atom (B or D site) has an *unoccupied* surface state. The present LDOS result corresponds to a bias-dependent STM image. Actually, such a bias-dependent STM im-

age is observed experimentally (26) on the flat (non-stepped) region, the A and B sites in Fig. 4(d). Therefore, we concluded that such a bias-dependent STM image will be observed also in the stepped region, the C and D sites in Fig. 4(d). More quantitative discussions will appear elsewhere.

4. Summary

Practical methods of large-scale electronic structure were constructed and their foundation is to calculate (one-body) density matrix or Green function, instead of eigenstates. In the application of cleavage process of silicon, nanoscale defects, step and bending, were observed as well as elementary surface reconstruction processes. All the results are consistent to experiments qualitatively and quantitatively. Moreover, our simulation results predict a practical step structure with the bias dependency of its STM image.

Since the present method for large systems is a general quantum mechanical calculation, it has wide applications, not specific to silicon or cleavage. Processes of other nanoscale or 10-nm-scale systems are possible targets in future study.

Acknowledgements

Numerical calculation was partly carried out using the facilities of the Japan Atomic Energy Research Institute, the Research Center for Computational Science, Okazaki and the Institute for Solid State Physics, University of Tokyo.

References

[1] R. Car and M. Parrinello, Phys. Rev. Lett. **55**, 2471 (1985).
[2] W. Kohn, Phys. Rev. Lett. **76**, 3168 (1996).
[3] For reviews; G. Galli, Phys. Status Solidi B**217**, 231 (2000); S. Y. Wu and C. S. Jayamthi, Phys. Rep. **358**, 1 (2002).
[4] T. Hoshi, Y. Iguchi and T. Fujiwara, Phys. Rev. B**72**, 075323 (2005).
[5] T. Hoshi and T. Fujiwara, J. Phys. Soc. Jpn. **69**, 3773 (2000).
[6] T. Hoshi and T. Fujiwara, Surf. Sci. **493**, 659 (2001).
[7] T. Hoshi and T. Fujiwara, J. Phys. Soc. Jpn. **72**, 2429 (2003).
[8] M. Geshi, T. Hoshi, and T. Fujiwara, J. Phys. Soc. Jpn. **72**, 2880 (2003).
[9] R. Takayama, T.Hoshi, and T.Fujiwara, J. Phys. Soc. Jpn. **73**, 1519 (2004).
[10] R. Takayama, T. Hoshi, T. Sogabe, S.-L. Zhang and T. Fujiwara, preprint (cond-mat/0503394).
[11] The program code for calculating Green function is available at http://act.jst.go.jp.
[12] I. Kwon, R. Biswas, C. Z. Wang, K. M. Ho, and C. M. Soukoulis, Phys. Rev. B **49**, 7242 (1994).
[13] Krylov subspace is a general mathematical concept in linear algebra. As a recent textbook, H. A. van der Vorst, *Iterative Krylov methods for large linear systems*, Cambridge University Press (2003).
[14] O. K. Andersen and O. Jepsen, Phys. Rev. Lett. 53, 2571 (1984).
[15] See Refs. (37-42) of Ref. (4)
[16] N. F. Mott, Engineering 165, 16 (1948).
[17] As a textbook, B. Lawn, *Fracture of brittle solids*, 2nd ed., Cambridge University Press (1993).
[18] Y. M. Huang, J. C. H. Spence, O. F. Sankey, and G. B. Adams, Surf. Sci. **256**, 344 (1991); J. C. H. Spence, Y. M. Huang, and O. Sankey, Acta Metall. Mater. **41**, 2815 (1993).
[19] R. Pérez and P. Gumbsch, Phys. Rev. Lett. **84**, 5347 (2000).
[20] J. A. Hauch, D. Holland, M. P. Marder and H. L. Swinney, Phys. Rev. Lett. 82, 3823 (1999).
[21] K. C. Pandey, Phys. Rev. Lett. **47**, 1913 (1981).
[22] See References in Ref. (4)
[23] R. M. Feenstra and J. A. Stroscio, Phys. Rev. Lett. **59**, 2173 (1987).
[24] H. Tokumoto, S. Wakiyama, K. Miki, H. Murakami, S. Okayama, and K. Kajimura, J. Vac. Sci. & Technol. B **9** 695 (1991); T. Komeda, S. Gwo, and H. Tokumoto, Jpn. J. Appl. Phys. **35**, 3724 (1996).
[25] Y. Mera, T. Hashizume, K. Maeda, and T. Sakurai, Ultramicroscopy **42-44**, 915 (1992).
[26] R. M. Feenstra, W. A. Thompson and A. P. Fein Phys. Rev. Lett. **56**, 608 (1986); J. A. Stroscio, R. M. Feenstra and A. P. Fein Phys. Rev. Lett. **57**, 2579 (1986).